Streamer propagation in the atmosphere of Titan and other N_2:CH_4 mixtures compared to N_2:O_2 mixtures

Köhn, Christoph; Dujko, Saša; Chanrion, Olivier; Neubert, Torsten

Published in:
Icarus

Link to article, DOI:
10.1016/j.icarus.2019.05.036

Publication date:
2019

Document Version
Publisher's PDF, also known as Version of record

Citation (APA):
Köhn, C., Dujko, S., Chanrion, O., & Neubert, T. (2019). Streamer propagation in the atmosphere of Titan and other N_2:CH_4 mixtures compared to N_2:O_2 mixtures. *Icarus*, *333*, 294-305. https://doi.org/10.1016/j.icarus.2019.05.036

Icarus 333 (2019) 294–305

Contents lists available at ScienceDirect

Icarus

journal homepage: www.elsevier.com/locate/icarus

Streamer propagation in the atmosphere of Titan and other N_2:CH_4 mixtures compared to N_2:O_2 mixtures

Christoph Köhn[a,*], Saša Dujko[b], Olivier Chanrion[a], Torsten Neubert[a]

[a] Technical University of Denmark, National Space Institute (DTU Space), Elektrovej 328, Kgs Lyngby 2800, Denmark
[b] Institute of Physics, University of Belgrade, Pregrevica 118, Belgrade 11080, Serbia

ABSTRACT

Streamers, thin, ionized plasma channels, form the early stages of lightning discharges. Here we approach the study of extraterrestrial lightning by studying the formation and propagation of streamer discharges in various nitrogen-methane and nitrogen-oxygen mixtures with levels of nitrogen from 20% to 98.4%. We present the friction force and breakdown fields E_k in various N_2:O_2 (Earth-like) and N_2:CH_4 (Titan-like) mixtures. The strength of the friction force is larger in N_2:CH_4 mixtures whereas the breakdown field in mixtures with methane is half as large as in mixtures with oxygen. We use a 2.5 dimensional Monte Carlo particle-in-cell code with cylindrical symmetry to simulate the development of electron avalanches from an initial electron-ion patch in ambient electric fields between $1.5E_k$ and $3E_k$. We compare the electron density, the electric field, the front velocities as well as the occurrence of avalanche-to-streamer transition between mixtures with methane and with oxygen. Whereas we observe the formation of streamers in oxygen in all considered cases, we observe streamer inceptions in methane for small percentages of nitrogen or for large electric fields only. For large percentages of nitrogen or for small fields, ionization is not efficient enough to form a streamer channel within the length of the simulation domain. In oxygen, positive and negative streamers move faster for small percentages of nitrogen. In mixtures with methane, electron or streamer fronts move 10–100 times slower than in mixtures with oxygen; the higher the percentage of methane, the faster the fronts move. On Titan with methane percentages between 1.4% and 5%, a successful streamer inception would require a large electric field of 4.2 MV m^{-1} ($3E_k$). Such large fields might not be present and explain the non-detection of Titan lightning by the Cassini/Huygens mission.

1. Introduction

Lightning on Earth is a highly complex phenomenon involving physical processes on various spatial and temporal scales (Villanueva et al., 1994; Ebert et al., 2006; Ebert and Sentman, 2008; Luque and Ebert, 2012; Rakov, 2013; da Silva and Pasko, 2013) starting from electron avalanches and resulting in the formation of hot, conducting lightning leaders. The early stages of lightning discharges are formed by streamers, thin, ionized plasma channels (Loeb, 1939; Raether, 1939; Loeb and Meek, 1940; Morrow and Lowke, 1997; Ebert and Sentman, 2008; Luque et al., 2008; Liu et al., 2012; Qin and Pasko, 2014). Three necessary, yet not sufficient, conditions for the inception of streamers are the presence of initial free electrons with a sufficiently high density, a sufficiently high ambient electric field to accelerate electrons and an ambient gas as a source of new electrons to sustain the streamer discharge.

In our solar system, lightning activity has been detected on several planets. Whilst the occurrence of lightning on Venus is still a controversial question (Russell et al., 2007; Takahashi et al., 2008; Moinelo et al., 2016; Pérez-Invernón et al., 2016; Takahashi et al., 2018), we posses clear evidences of lightning in the atmospheres of the gas and ice giants. Since Voyager 1, every probe that has approached Jupiter has imaged lightning flashes from its night side. Lightning has also been identified on Jupiter by its very-low frequency (VLF) radio signatures (Vasavada and Showman, 2005; Yair et al., 2008) and recently at 600 MHz by the Juno Microwave Radiometer (Brown et al., 2018). On Saturn, lightning has been recently detected optically and by its high-frequency (HF) radio signals (Dyudina et al., 2010, 2013), known as Saturn electrostatic discharges (SED) (Fischer et al., 2008). HF radio signals similar to those observed on Saturn have been detected by the Voyager 2 radio instrument at Uranus (Yair et al., 2008; Zarka and Pedersen, 1986). Lightning is also believed to take place at Neptune, based on the detection of lightning whistler like events observed during the encounter of Voyager 2 with this planet (Gurnett et al., 1990; Gibbard et al., 1999), and on Mars, in dust storms, based on the measurements of higher order moments of the electric field by a detector installed on NASA's Deep Space Network (Renno et al., 2003; Ruf et al., 2009) and supported by simulations by Melnik and Parrot (1998). However, more recent measurements on Mars by Anderson et al. (2012) and by Gurnett et al. (2010) using the Allen Telescope and the radar receiver of Mars Express have not found any signatures of lightning discharges. Hence, it is still controversial whether lightning exists on Mars.

The existence of atmospheric electric discharges on these planets

* Corresponding author.
E-mail address: koehn@space.dtu.dk (C. Köhn).

https://doi.org/10.1016/j.icarus.2019.05.036
Received 10 December 2018; Received in revised form 22 May 2019; Accepted 24 May 2019
Available online 14 June 2019

has been modelled by numerical simulations and tested by laboratory experiments. Using Monte Carlo simulations, Dwyer et al. (2006) simulated the runaway breakdown, which is the discharge initiation through high-energy electrons whose friction is significantly smaller than for low-energy electrons (Gurevich et al., 1992), in the atmospheres of Jupiter and Saturn. They found that the runaway breakdown field lowered by the presence of hydrometeors is ten times smaller than the conventional breakdown field and suggest that this might facilitate lightning inception on these planets.

Borucki et al. (1985) experimentally simulated lightning discharges on Venus, Jupiter and Titan by initiating laser-induced plasmas in various gas mixtures and found that the emitted spectral lines of these induced discharges depend significantly on the gas composition. On Jupiter, they mainly observed spectral lines associated with hydrogen whilst plasmas on Titan and Venus show spectral lines related to the abundance of the carbon molecules CH_4 and CO_2 as well as of atoms and ions related to nitrogen.

Dubrovin et al. (2010) investigated experimentally the inception and the motion of streamer discharges in CO_2:N_2 and H_2:He as they are present in the atmospheres of Venus and Jupiter above the cloud layers at pressures between 25 and 200 mbar. They discovered that streamer discharges similar to sprites could exist in these atmosphere, yet fainter than on Earth. However, to the best of our knowledge, there have not been any simulations of streamer discharges and their inception in non-terrestrial gas compositions modelling the very early stages of lightning discharges.

Amongst the bodies of our solar system, not only planets, but also some of their moons shelter an atmosphere, such as Jupiter's satellite Europa with a pressure of 10^{-11} bar (Hall et al., 1995) or Saturn's moon Titan. Both satellites are suspected to host amino acids (Raulin, 2005; Loison et al., 2015) which are a necessary condition for the formation of life as we know it (Haldane, 1929; Oparin, 1938; Ward and Kirschvink, 2015). Waite Jr. et al. (2007) discussed that cosmic gamma-rays enter Titan's atmosphere and facilitate the formation of organic compounds, so-called Tholins. Its atmosphere mainly consists of carbonaceous methane and nitrogen which resembles the atmosphere of the primordial Earth also containing carbon monoxide, water, methane and nitrogenous ammonia. Miller (1953) and Miller and Urey (1959) mimicked lightning by performing spark discharges in the same gas mixture as of primordial Earth. They discovered that amino acids were formed in their set-up concluding that lightning could be one trigger for the formation of life. Similarly, Plankensteiner et al. (2007) performed discharge experiments in a gas resembling the composition on Titan and found that possible discharges can produce higher hydrocarbons and molecules relevant for the formation of amino acids and nucleic acids.

First attempts to detect lightning on Titan were executed in 1980 when Voyager 1 flew by Saturn and Titan (Desch and Kaiser, 1990). Since the thickness of clouds and haze layers prevented the measurements of optical signatures, the search was extended towards spherics at radio wavelengths. However, no relevant data were recorded concluding that the maximum energy of a lightning flash on Titan would be approx. 1 MJ, approx. 1000 times weaker than for lighting flashes on Earth (Rakov and Uman, 2003).

In 2005, the Huygens Atmospheric Structure Instrument (HASI), designed to accurately measure atmospheric properties of Titan, measured a resonance at 36 Hz initially linked to the occurrence of lightning (Fulchignoni et al., 2005). Yet, a subsequent analysis of the provided data rather suggested that this resonance is an artifact of Titan's interaction with Saturn's magnetosphere (Béghin et al., 2009).

Successively, Cassini's RPWS (Radio and Plasma Wave Science) instrument (Lammer et al., 2001; Fischer et al., 2007; Lorenz and Mitton, 2008; Fischer and Gurnett, 2011) tried to search for radio emissions as an indicator for lightning on Titan during, in total, 127 flybys. Again, during these missions, no positive results were found; however, the conclusion was not that lightning does not exist on Titan, but rather that, if lightning exists, it is too weak to be detected.

Despite the fact that lightning has not been observed directly by cameras on-board or indirectly by radio instruments during Cassini's observations or during the descent of the Huygens probe, the atmospheric chemistry suggests the presence of electrical discharges in the atmosphere of Titan. Titan has a substantial atmosphere consisting predominantly of nitrogen and methane with trace amounts of hydrogen, hydrogen cyanide, ethane, propane, acetylene and other hydrocarbons and nitriles. The presence of the majority of these hydrocarbons and nitriles in the atmosphere of Titan has been explained in terms of photochemistry and charged-particle chemistry models with few exceptions. Perhaps the best known example is ethylene, which is more abundant in the upper atmosphere of Titan than photochemistry models would predict (Bar-Nun and Podolak, 1979; Borucki et al., 1988). Borucki et al. (1988) argued that the excess of ethylene in the upper Titan's atmosphere could be explained by upward diffusion of ethylene produced in the lower parts of the atmosphere by lightning. The post-Huygens era chemical model of Titan's atmosphere by Lavvas et al. (2008) still underestimates the abundance of ethylene in the stratosphere compared to the measurements. Likewise, the presence of acetylene and hydrogen cyanide with the relatively high abundances of $(1.9 \pm 0.2) \times 10^{-6}$ and $(1.5 \pm 0.2) \times 10^{-7}$ (Taylor and Coustenis, 1998), respectively, could also be explained by the lightning induced chemistry. On the contrary, more recent photochemical models (Vuitton et al., 2019) including isotopic photoabsorption and photodissociation for N_2 as well as photodissociation branching ratios for CH_4 and C_2H_2 simulates the density of organic species in Titan's atmosphere without the need of lightning discharges.

Whereas Earth's surface conductivity is approximately $10^{-14}\,\mathrm{S\,m^{-1}}$ (Wåhlin, 1994), Molina-Cuberos et al. (2001) approximated Titan's surface conductivity to range between $10^{-15}\,\mathrm{S\,m^{-1}}$ and $10^{-10}\,\mathrm{S\,m^{-1}}$, thus sufficiently large to allow the generation of cloud-to-ground lightning flashes. Tokano et al. give an extensive overview of available cloud convection and charging models as well as particle charging mechanisms (see Tokano et al., 2001 and references therein). They apply a one-dimensional time-dependent thundercloud model and state that negative space charges resulting from the attachment of electrons to clouds, can temporally create electric fields of up to $2\,\mathrm{MV\,m^{-1}}$ which is sufficient to initiate 20 km long negative cloud-to-ground lightning.

We here strive to answer the question whether streamer discharges, the pre-cursors of lightning, exist in Titan's atmosphere. Therefore, we perform Monte Carlo particle-in-cell simulations of electron avalanches in mixtures of N_2:CH_4 with different percentages of nitrogen in various electric fields and determine for which conditions the electron avalanches transition into streamer discharges. We also run simulations in N_2:O_2 mixtures with the same percentage of nitrogen and compare results for methane and for oxygen.

In Section 2 we briefly discuss the atmospheric profile of Titan and the set-up of our simulations. Additionally, we discuss the friction forces as well as the electric breakdown fields in different N_2:O_2 and N_2:CH_4 mixtures. In Section 3 we discuss the temporal evolution of the electron densities, the front velocities and the resulting electric field and compare results in mixtures with methane and with oxygen. We discuss when avalanche-to-streamer transitions are feasible and relate our results to the friction force and thus to the electron energy distribution. In Section 4 we summarize our results and discuss whether lightning is possible to occur on Titan. Finally, we give an outlook on future research activities.

2. Modelling and properties of Titan's atmosphere

2.1. Set-up of the model

We simulate the development of electron avalanches and, if existent, of subsequent streamers with a 2.5D Monte Carlo particle-in-cell code with cylindrical symmetry with two spatial coordinates (r,z) and

three coordinates (v_r,v_θ,v_z) in velocity space for each individual (super) electron (Chanrion and Neubert, 2008, 2010). We perform simulations in mixtures of N_2:O_2 and of N_2:CH_4 with different percentages κ of N_2. Thus, Earth's atmosphere is determined by $\kappa = 0.8$ with its nitrogen-oxygen mixture and Titan's atmosphere by $\kappa = 0.984$ with its nitrogen-methane mixture. For a better comparison of the results in different gas mixtures, we use a gas density of $2.9 \cdot 10^{25}\,\mathrm{m}^{-3}$ in all mixtures (see Section 2.2). As common for streamer discharges on Earth at different altitudes (Liu and Pasko, 2004), we here neglect external influences and concentrate on pure electron and streamer dynamics. Environmental influences such as the attachment to haze particles need a more extensive study after general avalanche and streamer characteristics in various N_2:O_2 and N_2:CH_4 have been discussed in the present paper.

The collision of electrons with nitrogen and oxygen molecules, cross sections as well as their implementation have already been studied carefully in various publications (e.g. Gurevich, 1961; Phelps and Pitchford, 1985; Crompton, 1994; Moss et al., 2006; Chanrion and Neubert, 2008; Dujko et al., 2011; Li et al., 2012; Köhn and Ebert, 2014, 2015). We review the collisions of electrons with methane molecules and the resulting friction force in Section 2.3.

Accounting for space charge effects, we solve the Poisson equation in the simulation domain with dimensions (L_r,L_z) = (1.25,14) mm and with 150 grid points in r- and 1200 grid points in z-direction (Köhn et al., 2017). As boundary conditions, we use Neumann conditions $\partial\phi/\partial r = 0$ for $r = 0,L_r$, and Dirichlet conditions for the electric potential $\phi(r,0) = 0$ and $\phi(r,L_z) = \phi_{max} = E_{amb} \cdot L_z$ where E_{amb} is the ambient electric field pointing downwards. We have performed simulations in ambient fields of 1.5, 2 and 3 times the classical breakdown field E_k.

We initiate all simulations with a charge neutral electron-ion patch at the center of the simulation domain. The initial electron density is given by the Gaussian $n_e(r, z, t = 0) = n_{e,0} \exp(-(r^2 + (z - z_0)^2)/\lambda^2)$ with $n_{e,0} = 10^{20}\,\mathrm{m}^{-3}$ as in Arrayás et al. (2002), Liu and Pasko (2004), and Köhn et al. (2017) and $\lambda = 0.2$ mm centered at $z_0 = 7$ mm. As in previous work, the initial electron energy is zero. As Li et al. (2007) have shown in a mixture of N_2:O_2 with $\kappa = 0.8$, electron energies equilibrate towards similar energy distributions for different initial electron energies below 50 eV.

2.2. Titan's atmospheric composition

An overview of the abundances of the constituents of Titan's atmosphere is given in Niemann et al. (2005). Titan's atmosphere is composed mainly of nitrogen and of methane where the percentage of methane varies from approx. 5% at ground up to approx. 1.4% at 140 km altitude. In order to perform reliable simulations, it is, however, not sufficient to know the gas composition, but we also need to specify the correct number density of ambient gas molecules. Lindal et al. (1983) and McKay et al. (1989) give an extended overview of Titan's temperature and pressure profile as a function of altitude. Further measurements of the temperature and pressure were later performed by the Huygens Atmospheric Structure Instrument (HASI) descending towards Titan's surface (Fulchignoni et al., 2005).

On Titan, clouds form between 20 km and 35 km altitude (Barth and Rafkin, 2007; Griffith et al., 2009) with the pressure varying between approximately 0.1 bar and 0.6 bar, the temperature varying between 70 K and 75 K and the level of methane varying between 1.6% and 2.0% (Müller-Wodrag et al., 2014). Hence, we here choose 1.6% of methane as well as $p = 0.3$ bar and $T = 75$ K yielding a gas density of $n_{Titan} = p/(k_B T) \approx 2.9 \cdot 10^{25}\,\mathrm{m}^{-3}$ using the ideal gas law. On Earth a density of $2.9 \cdot 10^{25}\,\mathrm{m}^{-3}$ corresponds to a pressure of approx. 1.2 bar at 300 K or approx. 1 bar at 250 K (equivalent to 10 km altitude).

2.3. Cross sections and friction forces for electrons in N_2:O_2 and N_2:CH_4 mixtures

Fig. 1a shows the cross sections $\sigma_{i,j}$ for different collision processes j of electrons at different species i. As for oxygen, electrons scatter off methane elastically, excite, ionize or attach to it. The most frequent process below approximately 50 eV is elastic scattering followed by excitations (Šašić, O. et al., 2004). Since the ionization threshold energy is $E_b \approx 12.6$ eV, the ionization cross section starts to increase for energies above and becomes predominant above approximately 50 eV.

However, due to the lack of reliable data, we do not have differential cross sections for elastic and inelastic collisions, including those for ionization. However, as we discuss below, most of the electrons in the N_2:CH_4 simulations have energies below 50 eV. For such low energies, the collision dynamics is well described by the approximation of isotropic scattering. The isotropy of scattering may be assumed due to the fact that numerous elastic collisions generally randomize directions of electron motion and hence one could not see any significant effects of introducing the anisotropy of scattering. The determination of the momentum transfer cross section is usually performed under the assumption of anisotropy, so the cross section has this assumption inherently built into it. Of course, for higher electron energies the approximation of isotropic scattering is no more valid and the use of differential cross sections for electron scattering is mandatory (see for example a detailed discussion in Li, 2009). The energy W of secondary ionization electrons is determined uniformly randomly in $[0,E_{in} - E_b]$ where E_{in} is the kinetic energy of the incident electron. Subsequently, we apply the conservation of energy and momentum and determine (Köhn and Ebert, 2014; Celestin and Pasko, 2010) the scattering angle

$$\cos\Theta_{sca} = \sqrt{\frac{(E_{in} - W)(E_{in} + 2m_e c^2)}{E_{in}(E_{in} - W + 2m_e c^2)}} \tag{1}$$

of the incident electron and the emission angle

$$\cos\Theta_e = \sqrt{\frac{W(E_{in} + 2m_e c^2)}{E_{in}(W + 2m_e c^2)}}. \tag{2}$$

of the liberated electron with m_e being the electron's rest mass and c the speed of light. Note that these relativistic equations are valid also for non-relativistic electron energies.

Panels b and c in Fig. 1 show the friction force

$$F_R(E) = \sum_{i,j} n_i \sigma_{i,j}(E) \Delta E_{i,j}, \tag{3}$$

where n_i is the partial density [m^{-3}] of N_2, O_2 or CH_4, $\sigma_{i,j}$ is the total cross section for collision process j of electrons at molecule species i and $\Delta E_{i,j}$ the respective energy loss of electrons. The sum is taken over all involved molecule species i and over all involved inelastic collisions j. Note that excitations and ionization are the only processes below 100 eV contributing to the friction where the energy loss resulting from excitations is the threshold energy of the collision and the energy loss for ionization is $1/2(E_{in} - E_b)$. Panel b) shows the friction of electrons in different mixtures of N_2:O_2. The overall shape is similar irrespective of the percentage κ of nitrogen. However, the strength of excitational losses for energies below 1 eV increases with decreasing κ since the cross section and subsequently the contribution of excitations is higher for oxygen than for nitrogen. On the contrary, the contribution of excitations above 1 eV increases with increasing percentage of nitrogen. For $E \gtrsim 1$ eV, there is a resonance in the cross section of the vibrational states of excited nitrogen with threshold energies of approximately 2 eV (see for example Tab. 1 in Moss et al., 2006). For energies above approximately 10 eV, the friction forces for different κ align because the total ionization cross section and the corresponding energy loss are comparable for nitrogen and oxygen.

Panel c) shows the friction force for different N_2:CH_4 mixtures. For comparison, the dashed yellow and purple lines additionally show the friction force for N_2:O_2 with 20% and 80% nitrogen. Whilst the overall shape of the friction force is different than for N_2:O_2, we observe the same dependency on κ: Since the cross section for exciting methane for electron energies between 0.2 eV and 2 eV is larger than for nitrogen,

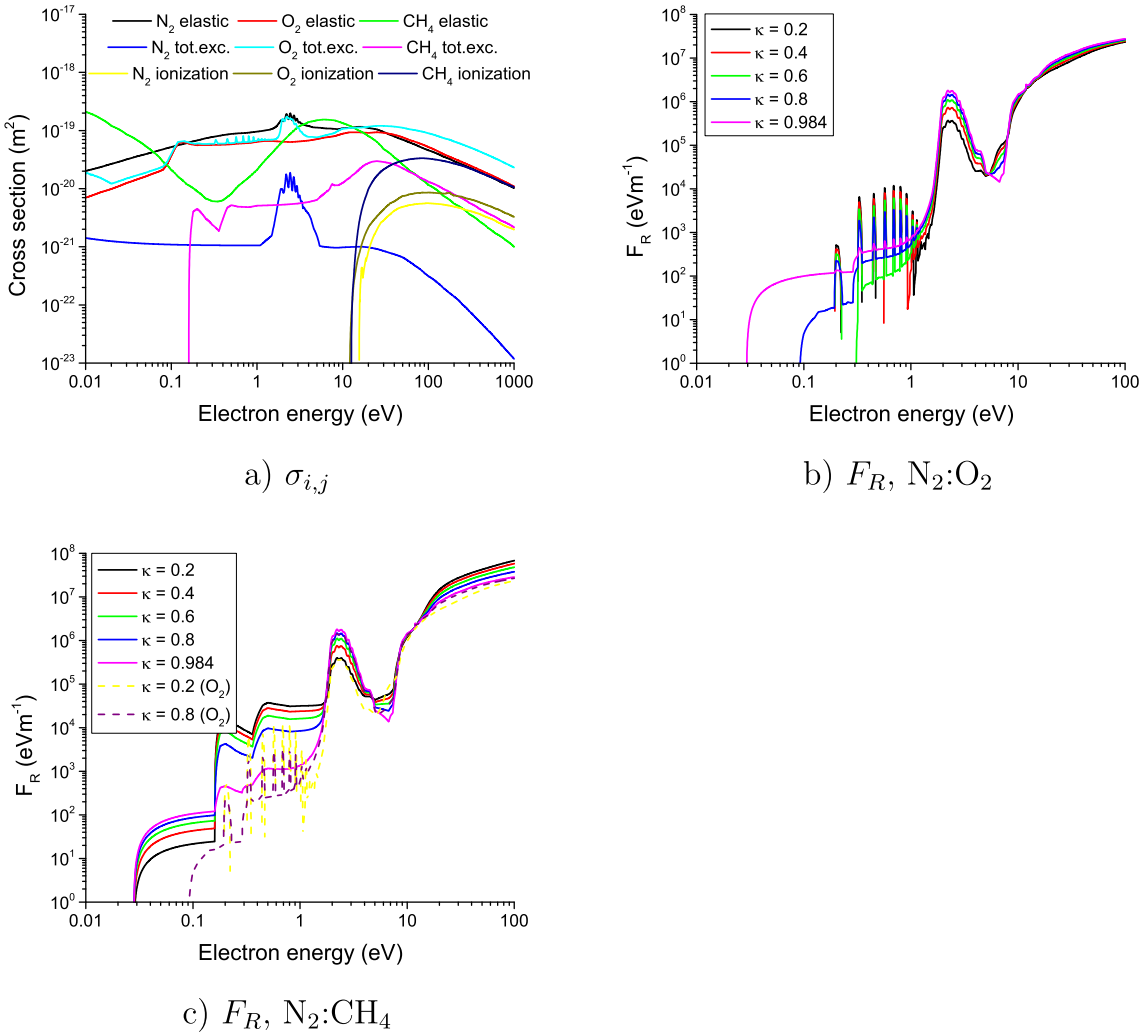

Fig. 1. a) Cross sections for electron scattering in N_2, O_2 and CH_4. We show cross sections for momentum transfer in elastic collisions, total cross sections for electronic excitation (including dissociation into neutral fragments) and cross sections for electron-impact ionization. b, c) The friction force in N_2:O_2 (b) and in N_2:CH_4 (c) as a function of electron energy for different percentages κ of molecular nitrogen. For comparison, the dashed yellow and purple lines in c) show the friction force for a N_2:O_2 mixture with 20% and 80% nitrogen. (For interpretation of the references to color in this figure legend, the reader is referred to the web version of this article.)

the friction force increases for an increasing percentage of methane. Because of the resonance of the cross section for exciting nitrogen above 2 eV, the friction increases with κ for energies between 2 eV and 5 eV. For energies above 5 eV, the friction increases and becomes smaller for large κ with an exception between 8 and 15 eV where the friction is almost independent of κ. Comparing the friction force in N_2:O_2 mixtures with the friction force in N_2:CH_4 mixtures reveals that, for fixed κ, the strength of the friction force above approximately 2 eV is similar for mixtures with oxygen and with methane, hence the energy loss of electrons above 2 eV is comparable. However, it is noticeable that for energies below 2 eV and fixed κ, the friction in N_2:CH_4 mixtures is approximately one to two orders of magnitude higher than in mixtures with oxygen.

2.4. Photoionization

In oxygen-nitrogen mixtures, one additional process contributing to the evolution of streamer discharges is photoionization: Electrons can excite nitrogen which subsequently emits UV photons. In return, these UV photons ionize oxygen and thus deliver a new source of electrons (Zheleznyak et al., 1982; Luque et al., 2007; Bourdon et al., 2007; Wormeester et al., 2010; Köhn et al., 2017). Although this process is not crucial for the development for negative fronts, it supports their motion (see e.g. a discussion in Luque et al., 2007; Köhn et al., 2017). For positive streamer fronts moving towards the cathode, however, photoionization is one of the key drivers next to background ionization (Pancheshnyi, 2005; Nijdam et al., 2011).

In oxygen, we use the model of Zheleznyak et al. (1982), Chanrion and Neubert (2008), and Köhn et al. (2017) which relates the number of UV photons with energies between 12.10 eV and 12.65 eV to the number of electron impact ionization. This is the energy range where photons do not interact with nitrogen and predominantly ionize molecular oxygen. Beyond 12.65 eV, photons mainly excite nitrogen and do not contribute to the ionization of oxygen anymore (Liu et al., 2012; Carter, 1972). The ionization energy of molecular nitrogen is 15.6 eV, thus larger than the upper limit for UV photoionization. Note that the threshold energy for the ionization of oxygen is 12.1 eV, thus on the lower limit of the energy of considered UV photons.

Since the ionization energy of methane is 12.6 eV, photoionization by UV photons still contributes to the development of electron avalanches or streamers in N_2:CH_4, even though less efficiently. We thus implement the model of Zheleznyak et al., but evaluate the UV photoionization process randomly in $(12.65 - 12.6)/(12.65 - 12.1) = 9\%$ of all photoionization events in the model by Zheleznyak et al. only,

which is the ratio of the energy intervals of UV photoionization in methane and in oxygen.

2.5. The electric breakdown field

During the motion of electrons through ambient gas, electrons undergo two competing processes: First, they gain energy through the background electric field and they lose energy through inelastic collisions with the ambient gas molecules. Second, amongst these inelastic collisions, electrons are capable of ionizing the ambient gas and multiply the total electron number as long as the primary electron's energy is above the ionization threshold energy. As a competing process, electrons attach to molecules reducing the total electron number. These two processes compete with each other and severely depend on the ambient electric field (Raizer, 1991). The breakdown (or critical) field E_k is defined as the electric field when the attachment rate equals the ionization rate. Thus, in order to initiate and sustain an electron avalanche and eventually transition into a streamer, electric fields at least above the breakdown field are required such that there is a sufficient number of ionization events.

All transport properties, including the ionization and attachment rates for electrons in N_2:O_2 and N_2:CH_4 mixtures, are calculated using a multi term theory for solving the Boltzmann equation (Dujko et al., 2010). The input data for the Boltzmann equation are the cross sections for electron scattering in N_2, O_2 and CH_4 presented in Section 2.3. The ionization coefficient is a monotonically increasing function of the electric field for both N_2:O_2 and N_2:CH_4 mixtures over the range of the electric fields considered in this work. On the other hand, the attachment coefficient firstly increases with the applied electric field, reaching a maximal value, and then it starts to decrease. As expected, we have found that the attachment rate is reduced for increasing concentration of N_2 in both N_2:O_2 and N_2:CH_4 mixtures over the entire range of electric fields considered. This follows from the fact that N_2 is a non-attaching gas. We have also found that the ionization rate is reduced for increasing concentration of N_2 in these mixtures. By increasing the nitrogen concentration, more and more inelastic channels are open, the electrons can lose several discrete values of energy in various inelastic collisions. Due to this inelastic cooling effect, the mean swarm energy is reduced and as a consequence, the ionization rate drops off. Finally, the ionization rate in the pure N_2 is less than the ionization rates in both O_2 and CH_4 over a range of the applied electric field which follow directly from the energy dependence of the cross sections for electron scattering. More details are described in the accompanying paper (Bošnjaković et al., 2019).

Fig. 2 shows the breakdown field as a function of the percentage κ of nitrogen for a density of $2.9 \cdot 10^{25}\,\mathrm{m}^{-3}$ as well as the ratio between the breakdown fields in N_2:O_2 and N_2:CH_4. It shows that in both gas mixtures, the breakdown field slightly decreases as a function of κ for $\kappa \leq 0.984$. It also shows that the ratio of the breakdown field in N_2:O_2 and in N_2:CH_4 is approximately 0.5 irrespective of κ although increasing for large κ. Whilst the electric field strength for breakdown varies between 3 and 4 MV m^{-1} in N_2:O_2, it amounts to only 1.5–2 MV m^{-1} in N_2:CH_4 mixtures.

3. Results

3.1. Temporal evolution of electron avalanches and streamers for different percentages of nitrogen

Under the influence of the ambient field the initial electron-ion patch first develops into an electron avalanche and eventually into a bidirectional streamer. The ambient electric field points downwards such that the negative front moves upwards whilst the positive front moves downwards. The attached video files show the temporal evolution of the electron density and the electric field for the gas mixtures with 20% and 1.6% methane.

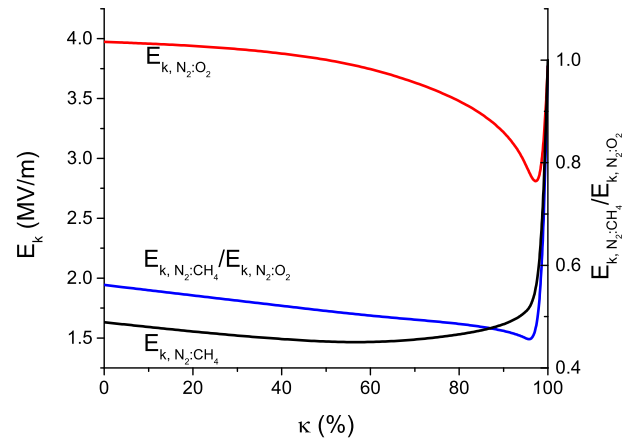

Fig. 2. The breakdown field E_k as a function of the percentage κ of nitrogen in N_2:O_2 mixtures and in N_2:CH_4 mixtures with a gas density of $2.9 \cdot 10^{25}\,\mathrm{m}^{-3}$. The plot also shows the ratio of the breakdown fields between these two different mixtures (right y-axis).

Fig. 3 shows the electron density and the electric field (third column) for gas mixtures with 80% nitrogen in ambient fields of $1.5E_k$ (first row), $2E_k$ (second row), $3E_k$ (third row), where E_k is ≈ 3.5 MV m^{-1} in mixtures with oxygen and ≈ 1.6 MV m^{-1} in mixtures with methane, after different time steps. In columns one to three, the left halves of each panel show the electron density or electric field in mixtures with 20% oxygen, i.e. the concentration on Earth, whereas the right halves show the density and field in mixtures with 20% methane which we refer to as Earth-like Titan. Fig. 4 shows the electron density in Earth-like Titan mixtures at the end of our simulations.

In our simulations, the electron-ion patch on Earth develops into a bidirectional streamer for any field above $1.5E_k$. The electric field shows the typical streamer-like pattern with an enhanced field at the tips and a shielded field inside the streamer body. Exchanging oxygen with methane dramatically changes the picture; the process of forming electron avalanches or eventually streamers becomes delayed significantly irrespective of the applied field. Columns one and two show that there is hardly any development whilst in mixtures with oxygen, streamers have already formed after the same time steps. However, the electric field shows the same pattern as in N_2:O_2 with an enhanced field at the tips of the electron patch and a vanishing shield in the patch's interior.

As Fig. 4 illustrates, we observe three different scenarios in mixtures with CH_4 at the end of the simulations depending on the ambient electric field. In a field of $1.5E_k$, the field at the positive front increases; however, the positive front does not move, hence there is no development of a positive streamer front. On the negative side, an electron avalanche, but no streamer front forms, without any significant field increase at the top. At the end of the simulation, the field at the tip is $1.8E_k$ and the electron density is $\lesssim 10^{17}\,\mathrm{m}^{-3}$. In an ambient field of $2E_k$, the situation does not change significantly at the positive front. The field increases, but the front does not develop. On the negative front, however, we observe the formation of a streamer-like channel. During the simulation, the field at the tip varies between approximately $3E_k$ and $6E_k$ whereas the field is shielded in its interior. In contrast to the density with $1.5E_k$ in Fig. 4a, the electron number slightly multiplies and reaches a density of $\approx 10^{19}\,\mathrm{m}^{-3}$ after 15.92 ns. In $E_{amb} = 3E_k$, there is the distinct formation of a positive and of a negative streamer front similar to as in air. Since the breakdown fields in N_2:O_2 and in N_2:CH_4 differ by a factor of ≈ 2, the absolute value of $3E_k$ in N_2:CH_4 corresponds to the value of $1.5E_k$ in air. Hence, the evolution of the electron density and of the electric field is comparable although delayed.

Fig. 5 shows the front velocities in the early stages of the evolution of electron avalanches and streamers for $\kappa = 0.8$ for O_2 and CH_4 and for

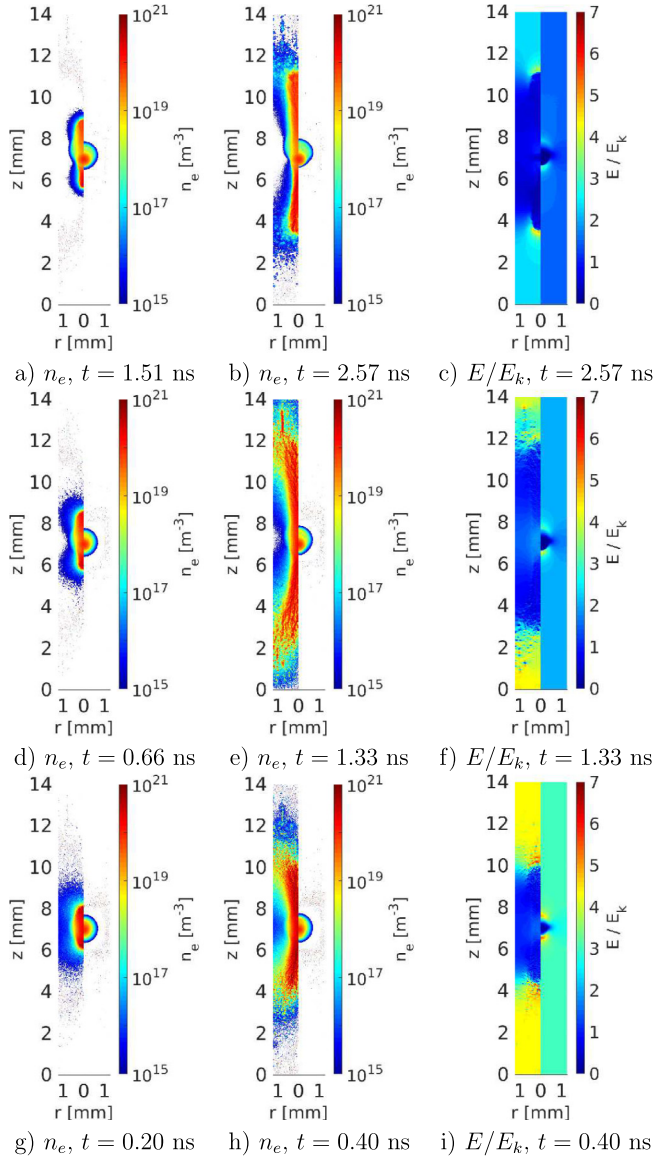

Fig. 3. The electron density n_e and the electric field E/E_k in the gas mixtures N_2:O_2 and N_2:CH_4 with 80% nitrogen in an ambient field of $1.5E_k$ (first row), $2E_k$ (second row) and $3E_k$ (third row). Columns 1 and 2 compare the electron density in mixtures with 20% oxygen (left half of each panel) with the density in mixtures with 20% methane (right half). Column 3 compares the electric field.

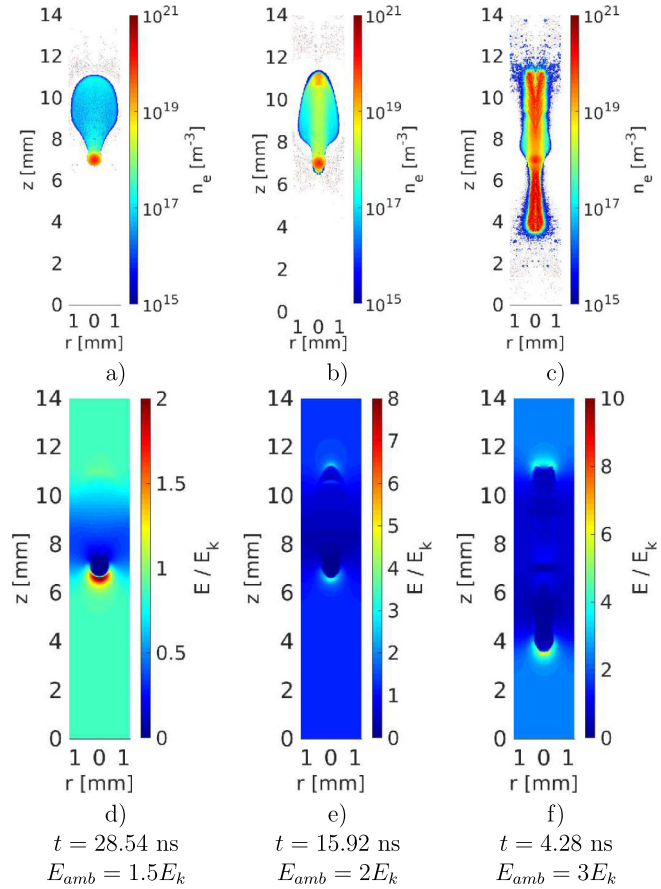

Fig. 4. The electron density n_e (first row) and the electric field (second row) in N_2:CH_4 with 80% nitrogen in different ambient fields at the end of the simulations.

all considered electric fields. Depending on the electric field, the streamer velocity in N_2:O_2 lies between 10^0 and 10^1 mm ns^{-1} and is similar for the positive and the negative streamer front. For $E_{amb} = 1.5E_k$ and $E_{amb} = 2E_k$ in N_2:CH_4 the velocity of the positive front lies between 10^{-2} and 10^{-1} mm ns^{-1} and is decreasing with time which is in agreement with panels a–c and d–f in Fig. 3 with no distinct fronts for these fields, similarly for negative fronts. For $3E_k$, Fig. 3i shows the development of a positive and a negative streamer front. The slope of the velocity is comparable to the increase of streamer velocities in air in a field of $1.5E_k$; however, in air, positive fronts and negative fronts are faster than in N_2:CH_4.

The delayed motion of fronts in mixtures with methane is related to the drift of electrons. Fig. 6a shows the drift velocity of electrons in nitrogen-methane and nitrogen-oxygen mixtures as a function of the ambient field. It is higher and increasing more significantly in mixtures with oxygen. Consequently the motion of fronts in N_2:CH_4 mixtures is delayed. Note that the calculation of the drift velocity does not consider space charges and therefore neglects the highly enhanced electric field in the streamer tips. Such high field tips usually accelerate electrons more efficiently than the ambient electric field which in turns lead to a higher velocity of streamer fronts than the electron drift velocity. In addition,a very steep gradient in the electron number density leads to a strong diffusive flux further enhancing the velocity of the propagating fronts. The differences in the avalanche-to-streamer transition as well as in the streamer evolution between Earth and Earth-like Titan for the same E_{amb}/E_k results from different ionization lengths in N_2:O_2 and in N_2:CH_4 as well as from the reduced probability for photoionization. Fig. 6b shows the effective ionization coefficient as a function of the electric field. It shows that ionization in a mixture with 20% methane is less effective than in a mixture with 20% oxygen for all considered field strengths. Beyond, the growth of the ionization coefficient is much less dominant in N_2:CH_4 mixtures than in N_2:O_2. Panel c) shows the ionization length Λ_{ion} as a function of E/E_k. In N_2:O_2 mixtures the ionization length varies from approximately 0.1 mm for $1.5E_k$ to 0.01 mm for $3E_k$ whilst it amounts to 4 mm for $1.5E_k$ in N_2:CH_4 mixtures with 80% nitrogen. Hence, in $1.5E_k$ in mixtures with methane, the ionization length is comparable to the size of the simulation domain preventing the occurrence of a significant amount of ionization. Since ionization is less effective in mixtures with methane, the build-up of space charges and thus the formation of enhanced electric field tips is delayed which reduces the electron energies and the further drive of ionization. Note that the ionization coefficient and the ionization length for $3E_k$ in N_2:CH_4 is comparable to the ionization coefficient for $1.5E_k$ in N_2:O_2.

For the same time steps and fields as in Figs. 3 and 4, panels a–c in Fig. 7 show the electron energy distribution. The solid and dashed lines show the typical streamer-like energy distributions of electrons in air

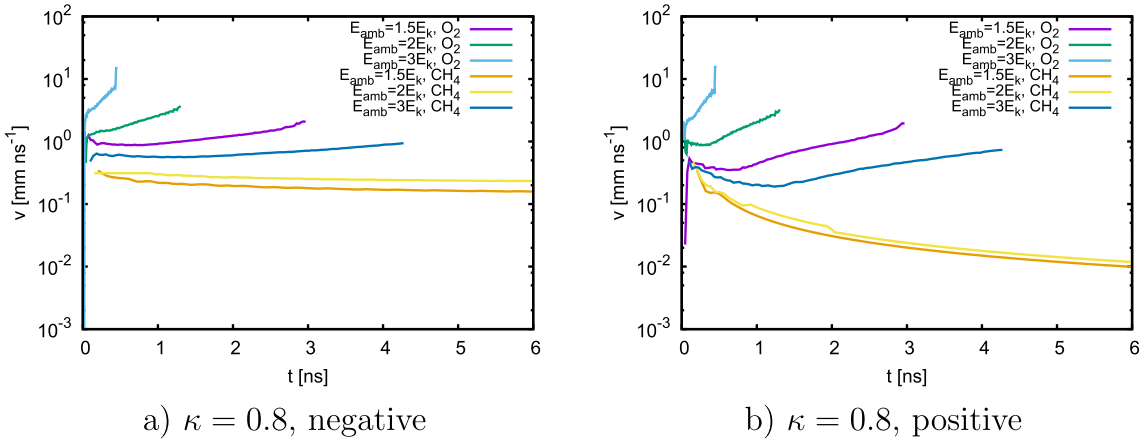

Fig. 5. The velocity of the positive (first column) and negative front (second column) as a function of time for gas mixtures with 80% nitrogen.

(Chanrion and Neubert, 2008) with maximum energies of ≈50 eV (1.5E_k, a), ≈65 eV (2E_k, b) and ≈80 eV (3E_k, c). However, for the same E_{amb}/E_k (remember that E_k is smaller in mixtures with methane), the maximum electron energies in N_2:CH_4 are ≈15 eV (a), ≈20 eV (b) and ≈30 eV (c), thus only a little above the ionization energy of nitrogen (15.6 eV) and of methane (12.6 eV). Hence, the ionization is not effective enough to create high field tips to accelerate electrons into the energy regime where they can further create a substantial electron multiplication. Comparing the electron numbers below 1 eV in N_2:CH_4 reveals that in an ambient field of 1.5E_k the electron number does not change significantly because of inefficient ionization whereas in a field of 3E_k. the electron number increases significantly as a function of time.

Fig. 8 shows the electron density and electric field in N_2:CH_4 with 20% nitrogen. It shows that in all considered cases negative and positive streamer fronts form. Fig. 7d compares the electron energy distribution for $\kappa = 0.2$ and $\kappa = 0.8$ for the same fields and time steps as in Fig. 8. It shows that in all cases, the maximum electron energy is larger for $\kappa = 0.2$ than for $\kappa = 0.8$ which results from the dependence of the friction force on the percentage of nitrogen. Fig. 1c shows that the friction force in N_2:CH_4 has a resonance at approximately 2 eV enhanced for $\kappa = 0.8$, reducing the electron energies. In addition, Fig. 2 shows that the breakdown field is slightly higher for $\kappa = 0.2$ than for $\kappa = 0.8$. Consequently, since the electron energies are larger for $\kappa = 0.2$, the ionization of the ambient gas is more probable and the

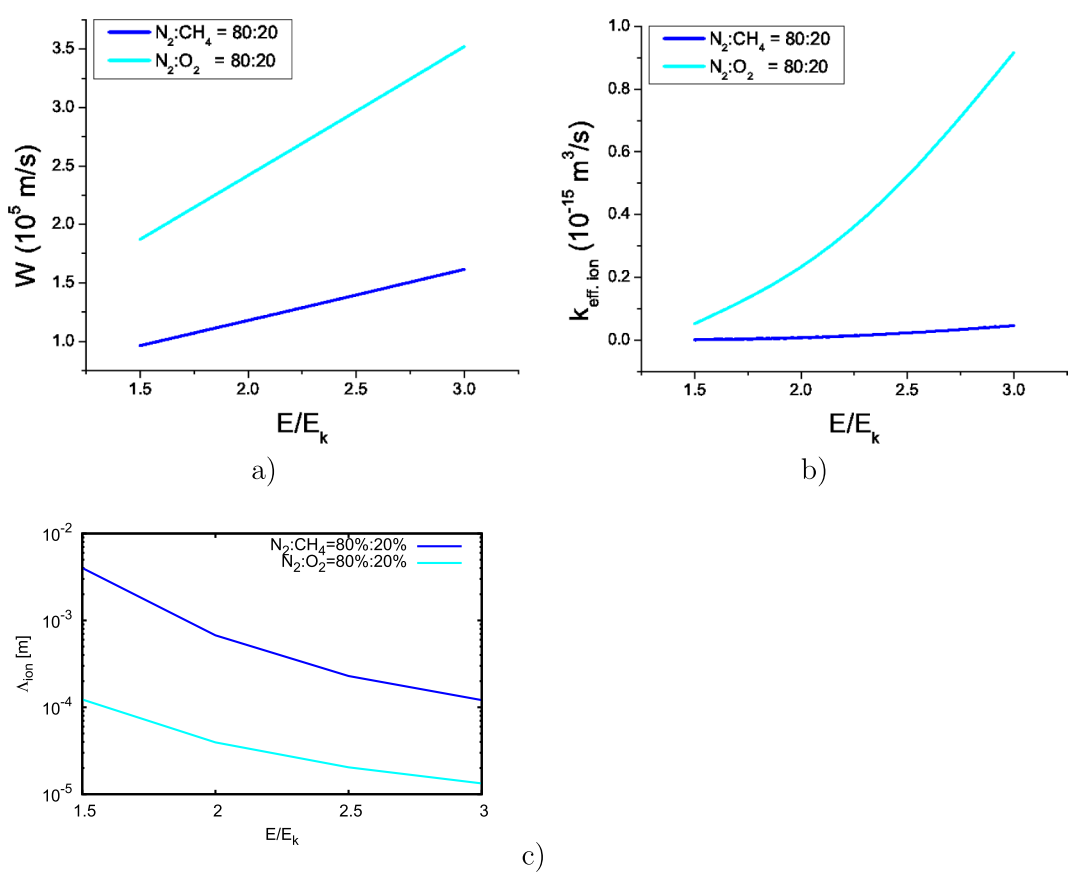

Fig. 6. The drift velocity (a), the effective ionization coefficient (b) and the ionization length Λ_{ion} (c) as a function of the ratio of the applied electric field and breakdown field.

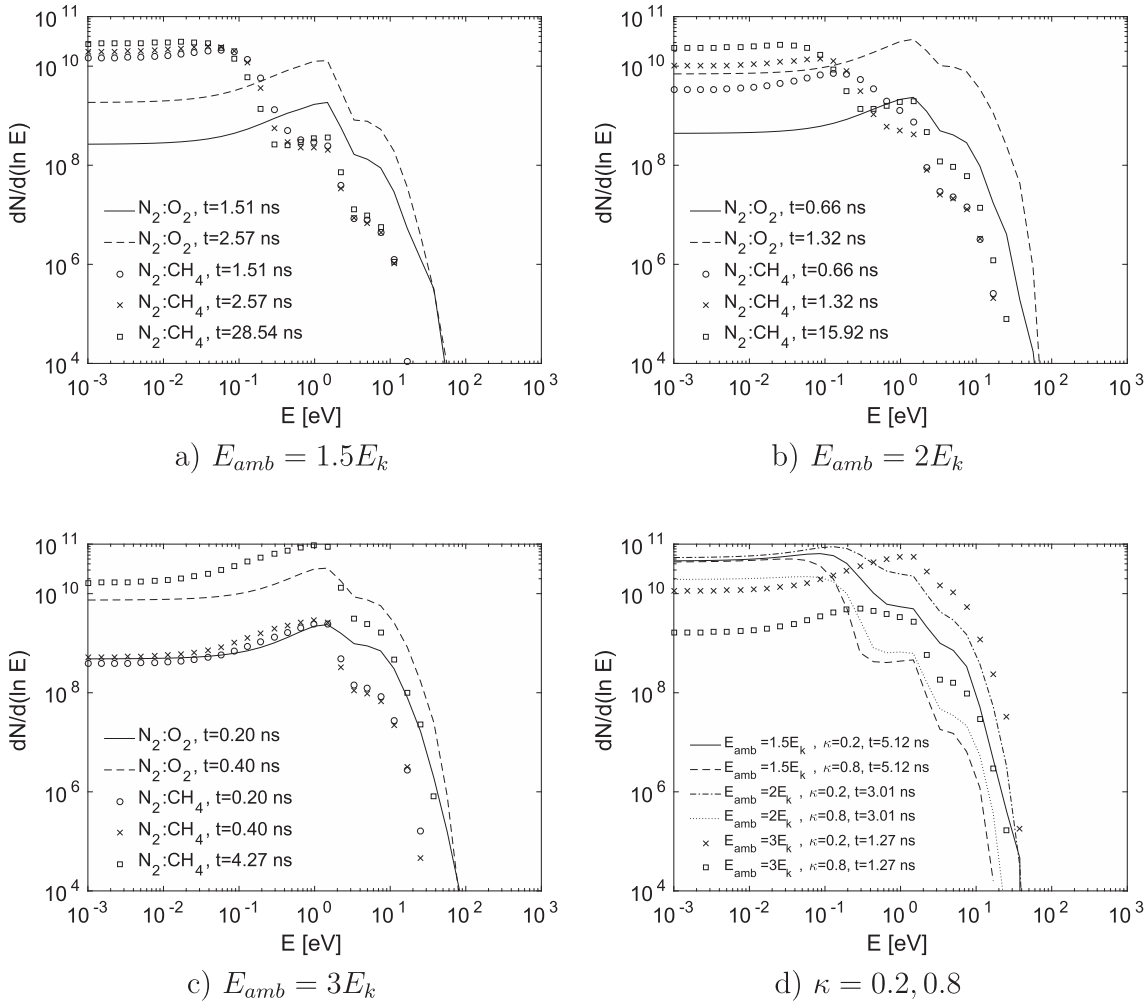

Fig. 7. The electron energy distribution in an ambient field of a) $1.5E_k$, b) $2E_k$ and c) $3E_k$ for $\kappa = 0.8$ after the same time steps as in Figs. 3 and 4. d) The energy distribution for $\kappa = 0.2$ and for $\kappa = 0.8$ for the same fields and time steps as in Fig. 8.

avalanche-to-streamer transition is facilitated.

For $\kappa = 0.2$, panels a and b in Fig. 9 show the streamer velocities in N_2:O_2 and N_2:CH_4 for all considered electric fields as a function of time. Although there is an avalanche-to-streamer transition for all field strengths, streamers move faster in oxygen than in methane. As for $\kappa = 0.8$, the streamer velocities equal $\approx 10^0$–10^1 mm ns^{-1} in oxygen whilst they lie between 10^{-1} and approximately 10^0 mm ns^{-1} in the nitrogen-methane mixture. Panels c) and d) additionally show the front velocities in N_2:CH_4 in an ambient field of $3E_k$ for different percentages of nitrogen. They illustrate that both positive and negative fronts move faster in mixtures with a low percentage of nitrogen or equivalently with a significant contribution of methane. Since the breakdown electric field does not vary much as a function of κ, we explain this with the friction force and its dependency on κ. As we have discussed in Section 2.3, the friction force has a resonance at an electron energy of approx. 2 eV which is distinct for large percentages of nitrogen. Subsequently, electron energies are lower and the fronts move slower in mixtures with high percentages of nitrogen. Equivalently fronts move substantially faster in mixtures with a significant concentration of methane.

3.2. The inception of streamers on Titan

After comparing the inception and evolution of bidirectional streamers in different N_2:CH_4 and N_2:O_2 mixtures, we now focus on the evolution of plasma patches and their transition to bidirectional streamers on Saturn's moon Titan, hence in N_2:CH_4 with 98.4% nitrogen. Fig. 10 shows the electron density and the electric field in different ambient fields; we here would like to remind the reader that the number density of ambient molecules is $2.9 \cdot 10^{25}\,\mathrm{m}^{-3}$ which corresponds to 20 km altitude on Titan, i.e. typical cloud altitudes in its atmosphere. As supplementary material, we have added movie files displaying the temporal evolution of the electron density and the electric field for the cases presented in Fig. 10. For comparison, the last column shows the electron density and the electric field in N_2:O_2 for the same number density of ambient gas molecules. Similar to $\kappa = 0.8$, we observe the avalanche-to-streamer transition in N_2:CH_4 only for fields above $2E_k$. As for $\kappa = 0.8$, the ionization length in fields below $2E_k$ is longer in mixtures with methane, thus the ionization is delayed and subsequently also the formation of enhanced field tips. In fields $\leq 2E_k$, there is a distinct motion of electrons towards the positive electrode only; there is no motion of the positive front at all. However, the field is enhanced at the positive front and shielded at the negative front suggesting that there will not be any avalanche-to-streamer transitions at later times. Fig. 11 shows the electron energies after the same time steps and in the same electric fields as in Fig. 10. The maximum electron energy is approximately 20 eV for fields smaller than $2E_k$ in N_2:CH_4, thus there is no efficient drive of ionization.

For fields above $2E_k$, we observe an avalanche-to-streamer transition within the borders of the simulation domain. However, comparing the evolution on Titan (third column) and in N_2:O_2 (fourth column), reveals that both streamer fronts move significantly slower in Titan's

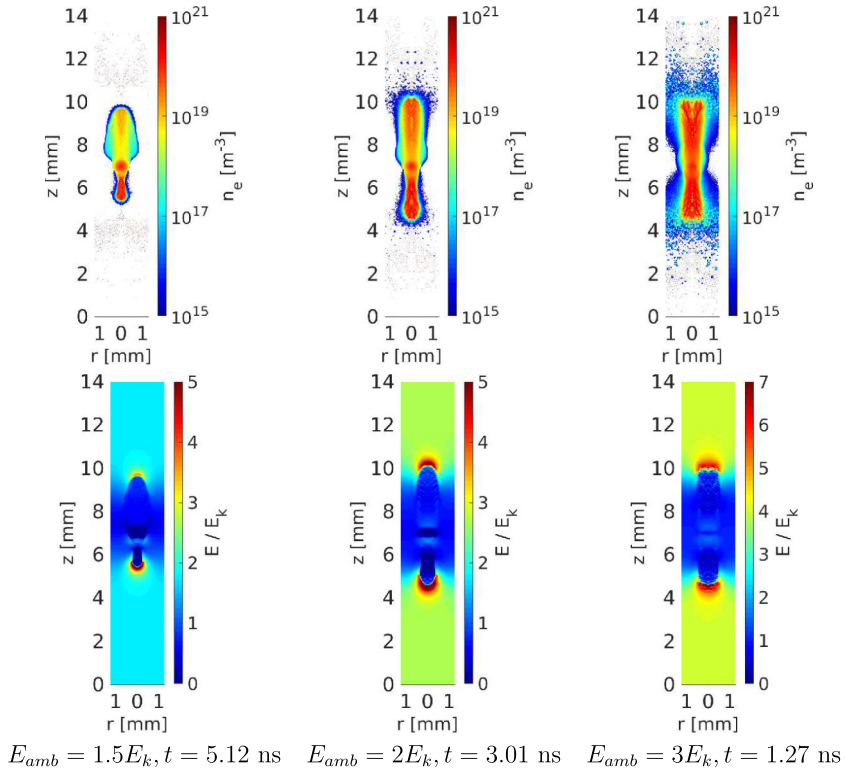

Fig. 8. The electron density (first row) and the electric field (second row) in N_2:CH_4 = (20%):(80%), i.e. $\kappa = 0.2$, in different electric fields after different time steps.

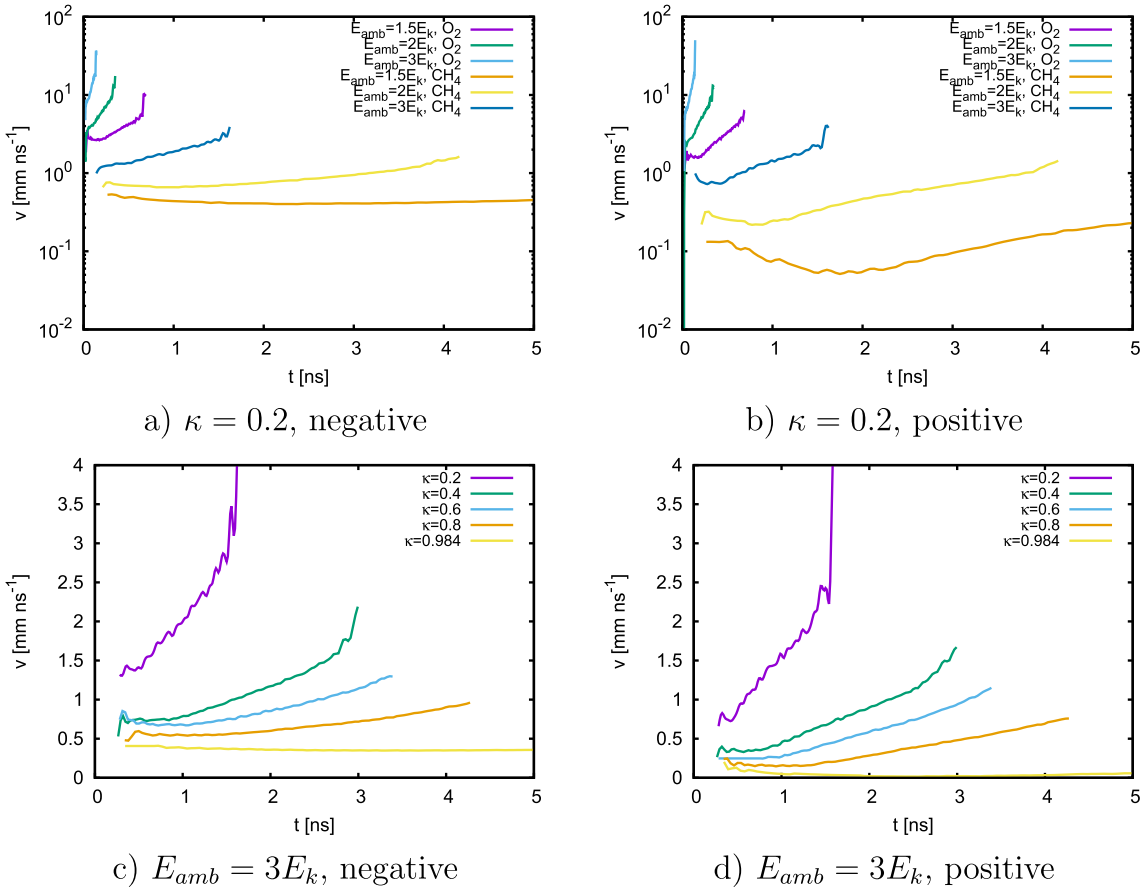

Fig. 9. a, b) The velocity of the negative (a) and positive front (b) as a function of time for gas mixtures with $\kappa = 0.2$ nitrogen. c, d) The velocity of the negative and of the positive front in N_2:CH_4 in an ambient field of $3E_k$ for different percentages of nitrogen.

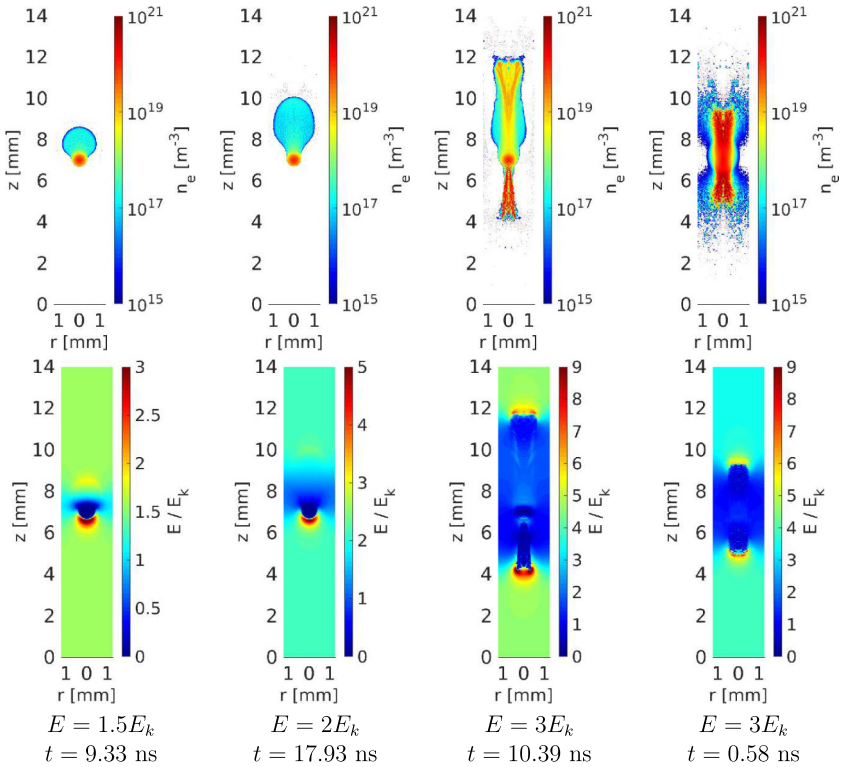

Fig. 10. The electron density (first row) and the electric field (second row) in N_2:CH_4 = (98.4%):(1.6%) (columns one to three) and in N_2:O_2 = (98.4%):(1.6%) (fourth column) in different ambient fields after different time steps.

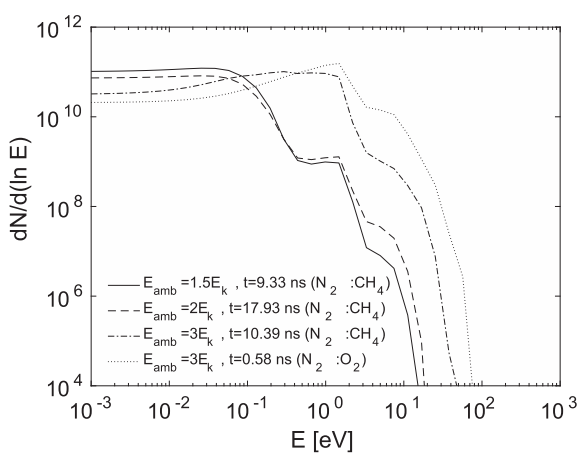

Fig. 11. The energy distribution for $\kappa = 0.984$ for the same fields and time steps as in Fig. 10.

atmosphere. Additionally, the electron density in N_2:CH_4 is smaller and branching is favored. The dot-dashed and dotted lines in Fig. 11 compare the electron energies for these two cases. There is a significant number of electrons above 20 eV resulting in more electron impact ionization. However, as a consequence of the friction force, the number of electrons above 20 eV is amplified in N_2:O_2 in comparison to N_2:CH_4 which accelerates the formation of a double-headed streamer. Furthermore, the less probable photoionization in N_2:CH_4 additionally delays the streamer development.

4. Conclusions and outlook

We have investigated the motion of electrons and the streamer inception in N_2:CH_4 and in N_2:O_2 mixtures with number densities of $2.9 \cdot 10^{25}\,\mathrm{m}^{-3}$ with different percentages κ of nitrogen in ambient fields of

Table 1
Criteria of successful avalanche-to-streamer transitions and subsequent streamer inception within the simulation domain with $L_z = 1.4$ cm in nitrogen-methane mixtures with different percentages κ of nitrogen in different ambient fields E_{amb}.

κ	E_{amb} $1.5E_k$	$2E_k$	$3E_k$
20%	✓	✓	✓
40%		✓	✓
60%		✓	✓
80%			✓
98.4%			✓

$1.5E_k$, $2E_k$ and $3E_k$. Whilst streamers form for all considered cases in N_2:O_2, we observe the streamer inception in N_2:CH_4 mixtures depending on κ and the ambient field E_{amb}. Table 1 shows which combinations of κ and E_{amb} favor the formation of double-headed streamers in N_2:CH_4 within the simulation domain. There are two scenarios: For small percentages of nitrogen, fields as low as $1.5E_k$ are sufficient to incept streamers; if the percentage of nitrogen is increased, higher and higher fields are required. Ambient fields slightly above the breakdown field, where the rate of ionization is higher than the rate for attachment, the effective ionization coefficient for large κ is not sufficient to effectively ionize the ambient gas within the simulation domain. For large percentages of nitrogen and small fields, the ionization length can be larger than or comparable to the size of the simulation domain preventing us from observing the inception of streamers.

Considering that for all κ, the breakdown field in N_2:CH_4 is approximately half as large as the breakdown field in N_2:O_2 and that the friction force below 3 eV is larger in N_2:CH_4, fronts move one to two orders of magnitude faster in nitrogen-oxygen mixtures than in nitrogen-methane mixtures independent of whether we observe an avalanche-to-streamer transition. As an additional effect, photoionization is less effective in N_2:CH_4, hence, the motion of the fronts is further

damped.

On Titan with methane percentages between 1.4% and 5%, we do not observe any streamer inception for ambient fields below $\approx 3E_k$ which equals a field strength of 4.2 MV m^{-1}. Simulations have calculated large scale electric fields as high as 2 MV m^{-1} in Titan's atmosphere (Tokano et al., 2001). Thus, at first glance it seems that streamer inception is not feasible in Titan's atmosphere. However, one may not forget that typical large scale electric fields in Earth's thunderclouds are typically in the order of 0.1–0.2 MV m^{-1} (Marshall et al., 1995, 2005) whereas the classical breakdown fields at cloud altitudes vary between approximately 2.0 MV m^{-1} at 4 km altitude and 0.5 MV m^{-1} at 16 km altitude, thus approximately an order of magnitude larger. Although the exact mechanism of lightning initiation on Earth is still under debate (Gurevich and Karashtin, 2013; Dubinova et al., 2015), its existence, and thus also streamer inception, are very well observed despite the difference between the large-scale thundercloud fields and the breakdown field. However, we note that the inception of streamers in Titan's atmosphere strongly depends on the ambient field which is still uncertain since it is only provided by models, but not by direct measurements. Moreover, even if we conclude the existence of small (cm-long) streamer discharges in Titan's atmosphere, this does not allow us to conclude about the existence of lightning. Although their existence cannot be ruled out completely, 127 flybys of Cassini did not reveal any traces of lightning (Fischer, 2018). Thus, either lightning was too weak to be detected (Fischer and Gurnett, 2011; Fischer, 2018), or it was not present at all because of the high field needed to incept streamers. Since even on Earth, the streamer-to-lightning-leader transition is not fully understood yet (da Silva and Pasko, 2013), we propose further work to study this transition in Titan's atmosphere.

Since the primordial atmosphere of Earth had a similar chemical composition as Titan's atmosphere, our model here allows us to also study the inception of streamers on the early Earth.

We here speculate that similar to the processes in terrestrial streamer discharges, run-away electrons and subsequently X-rays might be produced in Titan's atmosphere. In future work, we will estimate the occurrence and the fluence of these phenomena related to Titan γ-ray flashes (TGRFs) and discuss their effect on Titan's atmosphere.

The model presented in this manuscript also allows to study the streamer inception in different atmospheres, as for example, of exoplanets (Bailey et al., 2014; Hodosán et al., 2016a,b), provided appropriate cross sections for the scattering of electrons off the atmospheres' constituents are known. Hence, in future work, we strive to investigate which known exoplanets are likely to show discharge phenomena and also tackle the question of associated high-energy beams.

Acknowledgments

We would like to thank Georg Fischer from the Institut für Weltraumforschung (IWF), Graz, Austria, for fruitful discussions to improve the paper. The research was partly funded by the Marie Curie Actions of the European Union's Seventh Framework Programme (FP7/2007-2013) under REA grant agreement no. 609405 (COFUNDPostdocDTU). This project has received funding from the European Union's Horizon 2020 research and innovation programme under the Marie Sklodowska-Curie grant agreement 722337. SD acknowledges support from MPNTRRS Projects OI171037 and Ill41011.

Appendix A. Supplementary data

Supplementary data to this article can be found online at https://doi.org/10.1016/j.icarus.2019.05.036.

References

Anderson, M.M., Siemion, A.P.V., Barott, W.C., Bower, G.C., Delory, G.T., de Pater, I., Werthimer, D., 2012. The Allen Telescope Array search for electrostatic discharges on Mars. Astro. J. 744, 15.
Arrayás, M., Ebert, U., Hundsdorfer, W., 2002. Spontaneous branching of anode-directed streamers between planar electrodes. Phys. Rev. Lett. 88, 174502.
Bailey, R.L., Helling, C., Hodosán, G., Bilger, C., Stark, C.R., 2014. Ionization in atmospheres of brown dwarfs and extrasolar planets VI: properties of large-scale discharge events. Astro. J. 784, 43.
Bar-Nun, A., Podolak, M., 1979. The photochemistry of hydrocarbons in Titan's atmosphere. Icarus 38, 115–122.
Barth, E.L., Rafkin, S.C.R., 2007. TRAMS: a new dynamic cloud model for Titan's methane clouds. Geophys. Res. Lett. 34, L03203.
Béghin, C., Canu, P., Karkoschka, E., Sotin, C., Bertucci, C., Kurth, W.S., Berthelier, J.J., Grard, R., Hamelin, M., Schwingenschuh, K., Simões, F., 2009. New insights on Titan's plasma-driven Schumann resonance inferred from Huygens and Cassini data. Planet. Space Sci. 57, 1872–1888.
Borucki, W.J., Giver, L.P., McKay, C.P., Scattergood, T., Pariss, J.E., 1988. Lightning production of hydrocarbons and HCN on Titan: laboratory measurements. Icarus 76, 125–134.
Borucki, W.J., Mc Kenzie, R.L., McKay, C.P., Duong, N.D., Boac, D.S., 1985. Spectra of simulated lightning on Venus, Jupiter, and Titan. Icarus 64, 221–232.
Bourdon, A., Pasko, V.P., Liu, N.Y., Celestin, S., Ségur, P., Marode, E., 2007. Efficient models for photoionization produced by non-thermal gas discharges in air based on radiative transfer and the Helmholtz equations. Plasma Sour. Sc. Tech. 16, 656–678.
Bošnjaković, D., Simonović, I., Petrović, Z., Köhn, C., Duj-ko, S., 2019. Electron transport and propagation of negative planar ionization fronts in N_2:CH_4-mixtures. Unpublished manuscript. .
Brown, S., Janssen, M., Adumitroaie, V., Atreya, S., Bolton, S., Gulkis, S., Ingersoll, A., Levin, S., Li, C., Li, L., Lunine, J., Misra, S., Orton, G., Steffes, P., Tabataba-Vakili, F., Kolmasová, I., Imai, M., Santolík, O., Kurth, W., Hospodarsky, G., Gurnett, D., Connerney, J., 2018. Prevalent lightning sferics at 600 megahertz near Jupiter's poles. Nature 558, 87–90.
Carter, V.L., 1972. High-resolution N_2 absorption study from 730 to 980 Å. J. Chem. Phys. 56, 4195–4205.
Celestin, S., Pasko, V.P., 2010. Soft collisions in relativistic runaway electron avalanches. J. Phys. D: Appl. Phys. 43, 315206.
Chanrion, O., Neubert, T., 2008. A PIC-MCC code for simulation of streamer propagation in air. J. Comp. Phys. 227, 7222–7245.
Chanrion, O., Neubert, T., 2010. Production of runaway electrons by negative streamer discharges. J. Geophys. Res. 115, A00E32.
Wåhlin, L., 1994. Elements of fair weather electricity. J. Geophys. Res. 99, 10767–10772.
Crompton, R., 1994. Benchmark measurements of cross sections for electron collisions: electron swarm methods. Adv. Atom., Molecular Opt. Phys. 32, 97–148.
da Silva, C.L., Pasko, V.P., 2013. Dynamics of streamer-to-leader transition at reduced air densities and its implications for propagation of lightning leaders and gigantic jets. J. Geophys. Res. 118, 13561.
Desch, M.D., Kaiser, M.L., 1990. Upper limit set for level of lightning activity on Titan. Nature 343, 442–444.
Dubinova, A., Rutjes, C., Ebert, U., Buitink, S., Scholten, O., Trinh, G.T.N., 2015. Prediction of lightning inception by large ice particles and extensive air showers. Phys. Rev. Lett. 115, 015002.
Dubrovin, D., Nijdam, S., van Veldhuizen, E., Ebert, U., Yair, Y., Price, C., 2010. Sprite discharges on venus and jupiter-like planets: a laboratory investigation. J. Geophys. Res. 115, A00E34.
Dujko, S., Ebert, U., White, R., Petrović, Z.L., 2011. Boltzmann equation analysis of electron transport in a N_2-O_2 streamer discharge. Jpn. J. Appl. Phys. 50, 08JC01.
Dujko, S., White, R.D., Petrović, Z. Lj, Robson, R.E., 2010. Benchmark calculations of nonconservative charged-particle swarms in dc electric and magnetic fields crossed at arbitrary angles. Phys. Rev. E 81, 046403.
Dwyer, J.R., Coleman, L.M., Lopez, R., Saleh, Z., Concha, D., Brown, M., Rassoul, H.K., 2006. Runaway breakdown in the Jovian atmospheres. Geophys. Res. Lett. 33, L22813.
Dyudina, U.A., Ingersoll, A.P., Ewald, S.P., Porco, C.C., Fischer, G., Kurth, W.S., West, R.A., 2010. Detection of visible lightning on Saturn. Geophys. Res. Lett. 37, L09205.
Dyudina, U.A., Ingersoll, A.P., Ewald, S.P., Porco, C.C., Fischer, G., Yair, Y., 2013. Saturn's visible lightning, its radio emissions, and the structure of the 2009–2011 lightning storms. Icarus 226, 1020–1037.
Ebert, U., Montijn, C., Briels, T.M.P., Hundsdorfer, W., Meulenbroek, B., Rocco, A., van Veldhuizen, E.M., 2006. The multiscale nature of streamers. Plasma Sour. Sci. Technol. 15, 118–119.
Ebert, U., Sentman, D.D., 2008. Streamers, sprites, leaders, lightning: from micro- to macroscales. J. Phys. D: Appl. Phys. 41, 230301.
Fischer, G., 2018. Personal communication.
Fischer, G., Gurnett, D.A., 2011. The search for Titan lightning radio emissions. Geophys. Res. Lett. 38, L08206.
Fischer, G., Gurnett, D.A., Kurth, W.S., Akalin, F., Zarka, P., Dyudina, U.A., Farrell, W.M., Kaiser, M.L., 2008. Atmospheric electricity at saturn. Space Sci. Rev. 137, 271–285.
Fischer, G., Gurnett, D.A., Kurth, W.S., Farrell, W.M., Kaiser, M.L., Zarka, P., 2007. Nondetection of Titan lightning radio emissions with Cassini/RPWS after 35 close Titan flybys. Geophys. Res. Lett. 34, L22104.
Fulchignoni, M., Ferri, F., Angrilli, F., Ball, A.J., Bar-Nun, A., Barucci, M.A., Bettanini, C., Bianchini, G., Borucki, W., Colombatti, G., Coradini, M., Coustenis, A., Debei, S., Falkner, P., Fanti, G., Flamini, E., Gaborit, V., Grard, R., Hamelin, M., Harri, A.M., Hathi, B., Jernej, I., Leese, M.R., Lehto, A., Lion Stoppato, P.F., Lóópez-Moreno, J.J., Mäkinen, T., McDonnell, J.A.M., McKay, C.P., Molina-Cuberos, G., Neubauer, F.M.,

Pirronello, V., Rodrigo, R., Saggin, B., Schwingenschuh, K., Seiff, A., Simões, F., Svedhem, H., Tokano, T., Towner, M.C., Trautner, R., Withers, P., Zarnecki, J.C., 2005. In situ measurements of the physical characteristics of Titan's environment. Nature 438, 785–791.
Gibbard, S.G., Levy, E.H., Lunine, J.I., de Pater, I., 1999. Lightning on Neptune. Icarus 139, 227–234.
Griffith, C.A., Penteado1, P., Rodriguez, S., Le Mouéélic, S., Baines, K.H., Buratti, B., Clark, R., Nicholson, P., Jaumann, R., Sotin, C., 2009. Characterization of clouds in Titan's tropical atmosphere. ApJ Lett. 702, L105–L109.
Gurevich, A.V., 1961. On the theory of runaway electrons. Sov. Phys. JETP 12, 904–912.
Gurevich, A.V., Karashtin, A.N., 2013. Runaway breakdown in hydrometeors in lightning initiation. Phys. Rev. Lett. 110, 185005.
Gurevich, A.V., Milikh, G.M., Roussel-Dupré, R.A., 1992. Runaway electron mechanism of air breakdown and preconditioning during a thunderstorm. Phys. Lett. A 165, 463–468.
Gurnett, D.A., Kurth, W., Cairns, I.H., Granroth, L.J., 1990. Whistlers in Neptune's magnetosphere: evidence of atmospheric lightning. J. Geophys. Res. 95, 20967–20976.
Gurnett, D.A., Morgan, D.D., Granroth, L.J., Cantor, B.A., Farrell, W.M., Espley, J.R., 2010. Non-detection of impulsive radio signals from lightning in Martian dust storms using the radar receiver on the Mars Express spacecraft. Geophys. Res. Lett. 37, L17802.
Haldane, J., 1929. The origin of life. In: Rationalist Annual.
Hall, D.T., Strobel, D.F., Feldman, P.D., McGrath, M.A., Weaver, H.A., 1995. Detection of an oxygen atmosphere on Jupiter's moon Europa. Nature 373, 677–679.
Hodosán, G., Helling, C., Asensio-Torres, R., Vorgul, I., Rimmer, P.B., 2016a. Lightning climatology of exoplanets and brown dwarfs guided by solar system data. Monthly Not. Royal Astro. Soc. 461, 3927–3947.
Hodosán, G., Rimmer, P.B., Helling, C., 2016b. Is lightning a possible source of the radio emission on HAT-p_11b. Monthly Not. Royal Astro. Soc. 461, 1222–1226.
Köhn, C., Chanrion, O., Neubert, T., 2017. The influence of bremsstrahlung on electric discharge streamers in N_2, O_2 gas mixtures. Plasma Sour. Sci. Technol. 26, 015006.
Köhn, C., Ebert, U., 2014. The structure of ionization showers in air generated by electrons with 1 MeV energy or less. Plasma Sour. Sci. Technol. 23, 045001.
Köhn, C., Ebert, U., 2015. Calculation of beam of positrons, neutrons and protons associated with terrestrial gamma-ray flashes. J. Geophys. Res. Atmos. 120, 1620–1635.
Lammer, H., Tokano, T., Fischer, G., Stumptner, W., Molina-Cuberos, G.J., Schwingenschuh, K., Rucker, H.O., 2001. Lightning activity on Titan: can Cassini detect it? Planetary Space Sci. 49, 561–574.
Lavvas, P., Coustenis, A., Vardavas, I.M., 2008. Coupling photochemistry with haze formation in Titan's atmosphere, part II: results and validation with Cassini/Huygens data. Planet. Space Sci. 56, 67–99.
Li, C., 2009. Joining Particle and Fluid Aspects in Streamer Simulations. PhD thesis. Technical University of Eindhovenhttps://doi.org/10.6100/IR640104.
Li, C., Brook, W.J.M., Ebert, U., van der Mullen, J.J.A.M., 2007. Deviations from the local field approximation in negative streamer heads. J. Appl. Phys. 101, 123305.
Li, C., Ebert, U., Hundsdorfer, W., 2012. Spatially hybrid computations for streamer discharges: II. Fully 3D simulations. J. Comp. Phys. 231, 1020–1050.
Lindal, G.F., Wood, G.E., Hotz, H.B., Sweetnam, D.N., Eshleman, V.R., Tyler, G.L., 1983. The atmosphere of Titan: an analysis of the Voyager 1 radio occultation measurements. Icarus 53, 348–363.
Liu, N., Kosar, B., Sadighi, S., Dwyer, J.R., Rassoul, H.K., 2012. Formation of streamer discharges from an isolated ionization column at subbreakdown conditions. Phys. Rev. Lett. 109, 025002.
Liu, N., Pasko, V.P., 2004. Effects of photoionization on propagation and branching of positive and negative streamers in sprites. J. Geophys. Res. 109, A04301.
Loeb, L.B., 1939. Fundamental Processes of Electrical Discharges in Gases. Wiley, New York.
Loeb, L.B., Meek, J.M., 1940. The mechanism of spark discharge in air at atmospheric pressure. J. Appl. Phys. 11, 438–447.
Loison, J.C., Hébrard, E., Dobrijevic, M., Hickson, K.M., Caralp, F., Hue, V., Gronoff, G., Venot, O., Bénilan, Y., 2015. The neutral photochemistry of nitriles, amines and imines in the atmosphere of Titan. Icarus 247, 218–247.
Lorenz, R., Mitton, J., 2008. Titan Unveiled. Princeton University Press, New Jersey.
Luque, A., Ebert, U., 2012. Density models for streamer discharges: beyond cylindrical symmetry and homogeneous media. J. Comp. Phys. 231, 904–918.
Luque, A., Ebert, U., Montijn, C., Hundsdorfer, W., 2007. Photoionization in negative streamers: fast computations and two propagation modes. Appl. Phys. Lett. 90, 081501.
Luque, A., Ratushnaya, V., Ebert, U., 2008. Positive and negative streamers in ambient air: modeling evolution and velocities. J. Phys. D: Appl. Phys. 41, 234005.
Marshall, T.C., McCarthy, M.P., Rust, W.D., 1995. Electric field magnitudes and lightning initiation in thunderstorms. J. Geophys. Res. 100, 7097–7103.
Marshall, T.C., Stolzenburg, M., Maggio, C.R., Coleman, L.M., Krehbiel, P.R., Hamlin, T., Thomas, R.J., Rison, W., 2005. Observed electric fields associated with lightning initiation. Geophys. Res. Lett. 32, L03813.
McKay, C.P., Pollack, J.B., Courtin, R., 1989. The thermal structure of Titan's atmosphere. Icarus 80, 23–53.
Melnik, O., Parrot, M., 1998. Electrostatic discharge in Martian dust storms. J. Geophys. Res. 103, 29107–29118.
Miller, S.L., 1953. A production of amino acids under possible primitive earth conditions. Science 117, 3046.
Miller, S.L., Urey, H.C., 1959. Organic compound synthesis on the primitive Earth. Science 130, 3370.
Moinelo, A.C., Abildgaard, S., Muñoz, A.G., Piccioni, G., Grassi, D., 2016. No statistical evidence of lightning in Venus night-side atmosphere from VIRTIS-Venus Express Visible observations. Icarus 277, 395–400.
Molina-Cuberos, G.J., López-Moreno, J.J., Rodrigo, R., Schwingenschuh, K., 2001. Capability of the Cassini/Huygens PWA-HASI to measure electrical conductivity in Titan. Adv. Space Res. 28, 1511–1516.
Morrow, R., Lowke, J.J., 1997. Streamer propagation in air. J. Phys. D: Appl. Phys. 30, 614–627.
Moss, G.D., Pasko, V.P., Liu, N., Veronis, G., 2006. Monte Carlo model for analysis of thermal runaway electrons in streamer tips in transient luminous events and streamer zones of lightning leaders. J. Geophys. Res. 111, A20307.
Müller-Wodrag, I., Griffith, C.A., Lellouch, E., Cravens, T.E., 2014. Titan: Interior, Surface, Atmosphere and Space Environment. Cambridge University Press, New York.
Niemann, H.B., Atreya, S.K., Bauer, S.J., Carignan, G.R., Demick, J.E., Frost, R.L., Gautier, D., Haberman, J.A., Harpold, D.N., Hunten, D.M., Israel, G., Lunine, J.I., Kasprzak, W.T., Owen, T.C., Paulkovich, M., Raulin, F., Raaen, E., Way, S.H., 2005. The abundances of constituents of Titan's atmosphere from the GCMS instrument on the Huygens probe. Nature 438, 779–784.
Nijdam, S., Wormeester, G., van Veldhuizen, E.M., Ebert, U., 2011. Probing background ionization: positive streamers with varying pulse repetition rate and with a radioactive admixture. J. Phys. D: Appl. Phys. 44, 455201.
Oparin, A.I., 1938. The Origin of Life. Macmillan, New York.
Pancheshnyi, S., 2005. Role of electronegative gas admixtures in streamer start, propagation and branching phenomena. Plasma Sour. Sci. Technol. 14, 645–653.
Pérez-Invernón, F.J., Luque, A., Gordillo-Vázquez, F.J., 2016. Mesospheric optical signatures of possible lightning on Venus. J. Geophys. Res. Space Phys. 121, 7026–7048.
Phelps, A.V., Pitchford, L.C., 1985. Anisotropic scattering of electrons by N_2 and its effect on electron transport. Phys. Rev. A 31, 2932–2949.
Plankensteiner, K., Reiner, H., Rode, B.M., Mikoviny, T., Wisthaler, A., Hansel, A., Märk, T.D., Fischer, G., Lammer, H., Rucker, H.O., 2007. Discharge experiments simulating chemical evolution on the surface of Titan. Icarus 187, 616–619.
Qin, J., Pasko, V.P., 2014. On the propagation of streamers in electrical discharges. J. Phys. D: Appl. Phys. 47, 435202.
Raether, H., 1939. Die Entwicklung der Elektronen in den Funkenkanal. Z. Phys. 112, 464–489.
Raizer, Y.P., 1991. Gas Discharge Physics. Springer, Berlin.
Rakov, V.A., 2013. The physics of lightning. Surv. Geophys. 34, 701–729.
Rakov, V.A., Uman, M.A., 2003. Lightning: Physics and Effects. Cambridge Univ. Press, New York.
Raulin, F., 2005. Exo-astrobiological aspects of Europa and Titan: from observations to speculations. Space Sci. Rev. 116, 471–487.
Renno, N.O., Wong, A.S., Atreya, S.K., de Pater, I., Roos-Serote, M., 2003. Electrical discharges and broadband radio emission by Martian dust devils and dust storms. Geophys. Res. Lett. 30, 2140.
Ruf, C., Renno, N.O., Kok, J.F., Bandelier, E., Sander, M.J., Gross, S., Skjerve, L., Cantor, B., 2009. Emission of non-thermal microwave radiation by a Martian dust storm. Geophys. Res. Lett. 36, L13202.
Russell, C.T., Zhang, T.L., Delva, M., Magnes, W., Strangeway, R.J., Wei, H.Y., 2007. Lightning on Venus inferred from whistler-mode waves in the ionosphere. Nature 450, 661–662.
Takahashi, Y., Sato, M., Imai, M., Lorenz, R., Yair, Y., Aplin, K., Fischer, G., Nakamura, M., Ishii, N., Abe, T., Satoh, T., Imamura, T., Hirose, C., Suzuki, M., Hashimoto, G.L., Hirata, N., Yamazaki, A., Sato, T.M., Yamada, M., Murakami, S., Yamamoto, Y., Fukuhara, T., Ogohara, K., Ando, H., Sugiyama, K., Kashimura, H., Ohtsuki, S., 2018. Initiation of a lightning search using the lightning and airglow camera onboard the Venus orbiter Akatsuki. Earth, Planets and Space 70, 88.
Takahashi, Y., Yoshida, J., Yair, Y., Imamura, T., Nakamura, M., 2008. Lightning detection by LAC onboard the Japanese Venus Climate Orbiter. Planet-C. Space Sci. Rev. 137, 317–334.
Taylor, F.W., Coustenis, A., 1998. Titan in the solar system. Planet. Space Sci. 46, 1085–1097.
Tokano, T., Molina-Cuberos, G.J., Lammer, H., Stumptner, W., 2001. Modelling of thunderclouds and lightning generation on Titan. Planetary and Space Sci. 49, 539–560.
Vasavada, A.R., Showman, A.P., 2005. Jovian atmospheric dynamics: an update after Galileo and Cassini. Rep. Prog. Phys. 68, 1935–1996.
Villanueva, Y., Rakov, V.A., Uman, M.A., Brook, M., 1994. Microsecond-scale electric field pulses in cloud lightning discharges. J. Geophys. Res. 99, 14353–14360.
Šašić, O., Malović, G., Strinić, A., Nikitović, Z., Petrović, Z. Lj, 2004. Excitation coefficients and cross-sections for electron swarms in methane. New. J. of Phys. 6, 74.
Vuitton, V., Yelle, R.V., Klippenstein, S.J., Hörst, S.M., Lavvas, P., 2019. Simulating the density of organic species in the atmosphere of Titan with a coupled ion-neutral photochemical model. Icarus 324, 120–197.
Waite Jr., J.H., Young, D.T., Cravens, T.E., Coates, A.J., Crary, F.J., Magee, B., Westlake, J., 2007. The process of tholin formation in Titan's upper atmosphere. Science 316, 870–875.
Ward, P., Kirschvink, J., 2015. A New History of Life: The Radical Discoveries About the Origins and Evolution of Life on Earth. Bloomsbury Press.
Wormeester, G., Pancheshnyi, S., Luque, A., Nijdam, S., Ebert, U., 2010. Probing photoionization: simulations of positive streamers in varying N_2:O_2-mixtures. J. Phys. D: Appl. Phys. 43, 505201.
Yair, Y., Fischer, G., Simoes, F., Renno, N., Zarka, P., 2008. Updated review of planetary atmospheric electricity. Space Sci. Rev. 137, 29–49.
Zarka, P., Pedersen, B.M., 1986. Radio detection of uranian lightning by Voyager 2. Nature 323, 605–608.
Zheleznyak, M.B., Mnatsakanian, A.K., Sizykh, S.V., 1982. Photoionization of nitrogen and oxygen mixtures from a gas discharge. High Temp. 20, 357–362.